STM Studies on the Reconstruction of the $Ni_2P(10\bar{1}0)$ Surface

Donghui Guo[1], Yuta Nakagawa[2], Hiroko Ariga[1,5], Shushi Suzuki[3,5], Kumiko Kinoshita[4], Takeshi Miyamoto[2], Satoru Takakusagi[1,2,5] , Kiyotaka Asakura[1,2]*, Shigeki Otani[6], and S.Ted Oyama[7]

1. Section of Surface Structure Chemistry, Catalysis Research Center, Hokkaido University Sapporo 001-0021, Japan

2 Department of Quantum Science and Technology, Graduate School of Engineering, Hokkaido University, Kita 21-10, Kita-Ku Sapporo 001-0021, Japan

3 Department of Crystalline Materials Science, Graduate School of Engineering, Nagoya University, Furo-cho, Chikusa-ku Nagoya 464-8603, Japan

4 Environmental Material Development, Material Research and Development Laboratory, Japan Fine Ceramics Center, 2-4-1 Mutsuno, Atsuta, Nagoya, 456-8587, Japan

5 Research Cluster of Well-defined Surface Material, Catalysis Research Center, Hokkaido University Sapporo 001-0021, Japan

6 National Institute for Material Science, 1-1 Namiki, Tsukuba, Ibaraki 305

7 Environmental Catalysis and Nanomaterials Laboratory, Department of Chemical Engineering, Virginia Tech, Blacksburg, VA 2406, U.S.A.

Abstract

The surface structure of $Ni_2P(10\bar{1}0)$, a model for highly active hydrodesulfurization catalysts, was studied using scanning tunneling microscopy (STM) and low energy electron diffraction (LEED) in order to understand the reconstruction of the surface layers. Annealing at 573 K revealed a (1x1) LEED pattern which changed to a $c(2\times4)$ arrangement by further heating to 723 K. Atomic scale STM images were obtained for both the (1×1) and $c(2\times4)$ structures. Bright spots observed in the STM images were interpreted to be due to surface phosphorus atoms and this was supported by a density functional theory (DFT) simulation. Several possible models for the $c(2\times4)$ reconstructed structures were proposed including a P-dimer defect model, a missing-row model and a missing-row + added row model. The last model gave the best explanation for the $c(2\times4)$ structure. The mechanism for the c(2x4) reconstruction on the $Ni_2P(10\bar{1}0)$ surface is discussed.

1. Introduction

Nickel phosphide (Ni_2P) belongs to the class of metal-rich transition metal-main group element compounds (TM compounds), and has recently drawn much attention because of its high activity for hydrodesulfurization reactions [1,2]. Several surface science studies of Ni_2P single crystals have been conducted in order to elucidate the surface structure of Ni_2P and shed light on its high activity [3-9]. Much work has focused on the $Ni_2P(0001)$ surface which has two termination planes denoted as Ni_3P and Ni_3P_2, which are sequentially stacked in the crystal structure. The $Ni_2P(0001)$ surface also shows several reconstructed structures such as ($\sqrt{3} \times \sqrt{3}$)R 30°, (2/3×2/3) , and (2×2) [5,6] in addition to the primitive (1×1) structures. Since the reconstructed structures are energetically stable surfaces, it is important to determine the conditions at which they form to better understand the structure of real Ni_2P catalysts.

Surface reconstructions have often been found for metal, semiconductor and ionic crystals. The origins for reconstruction have been related to various physical properties of the crystals such as charge balance and dangling bonds or effects due to relativistic effects. The surfaces of late transition metal such as Ir, Pt and Au undergo reconstruction so as to give closed-packed structures as explained by Fiorentini et al [10] who claimed that relativistic effects induce the reconstruction of the 5d transition elements. For ionic compounds such as oxides and halides, surface charge balance or the reduction of dipole moments play an important role [11]. On a tetrahedral semiconductor surface, Duke suggested principles for the surface reconstructions [12-14].

TM phosphides usually have metallic conductivity and physical properties consistent with polar covalent bonds, and their bonding has been described as possessing metallic, ionic and covalent contributions. It is therefore quite interesting to consider what factors govern surface reconstruction of TM compounds. An impediment is that the surface structures of TM compounds have not been well studied, so that data are scarce and there are no general rules governing the reconstruction of TM compounds. Our previous studies have reported atomic level images of two types of ($\sqrt{3} \times \sqrt{3}$)R 30° reconstructed $Ni_2P(0001)$ [6]. As mentioned earlier, the $Ni_2P(0001)$ surface has two possible primitive surface terminations, i.e., Ni_3P and Ni_3P_2 that reflect their stoichiometry, but neither of which have the bulk Ni:P=2:1 ratio. (However, their sum, Ni_6P_3, does, as the terminations alternate and don't share atoms.) These $Ni_2P(0001)$ surface terminations are not the only stable structures, and reconstruction patterns are observed as noted before, which may be due to surface charge imbalances or the presence of surface dipoles, which have been evoked as important in the surface reconstruction of oxides [11,12]. In this study the structure of the $Ni_2P(10\bar{1}0)$ surface, which has a stoichiometric composition of Ni:P=2:1, was studied by low energy electron diffraction (LEED) and scanning tunneling microscopy (STM). Unexpectedly, it was found that the surface underwent reconstruction to a c(2×4) structure as determined by LEED. Determination of the real-space structure by STM

allowed the assessment of several possible model structures, leading to a possible principle for the reconstruction of Ni_2P surfaces.

2. Experimental

All experiments were performed in an Omicron ultra-high vacuum (UHV) system with a base pressure below 2 x 10^{-8} Pa. The system is equipped with an Omicron room temperature STM system, an Ar^+ sputtering gun (Omicron ISE5), a quadrupole mass spectrometer, four-grid reverse view LEED optics, and a gas handling system. The Ni_2P crystal was grown using a floating zone method under an Ar atmosphere with a growth speed of 1 cm/h. The Ni_2P $(10\bar{1}0)$ single crystal surface was cut and mechanically polished to a mirror finish. The sample was mounted on a sample holder and was fixed by spot welding to Tantalum ribbons which were used as electrodes for resistive heating. The sample was transferred to the UHV chamber and was cleaned by sputtering with 0.5 keV Ar^+ ions (current = 8μA, time = 5 min, Ar pressure = 2.5 x 10^{-3} Pa) and annealing in the UHV system at various temperatures. The STM images were measured at room temperature in a constant current mode. A W tip was used which was prepared by electrochemically etching in a 2N NaOH solution.

The STM images were simulated by DFT-GGA calculations of the local electron density of a six atom-layer slab of a Ni_2P $(10\bar{1}0)$ -(1x1) surface separated by a 2.5 nm vacuum gap. Since the STM images were mainly taken at negative bias conditions, the electron density was calculated for a range of 1.2 eV below E_F to E_F with heights of about 0.25 nm from the surface according to the Tersoff and Hamann method [15]. The *ab initio* calculations were performed with Wien2K code [16,17] and "GGA of Perdew-Burke-Ernzerhof 96" was used. The bulk-optimized structure was used without surface relaxationin order to compare the electron densities of Ni and P .

3.Results and Disccusion

3.1 LEED observations

Figure 1 shows the bulk Ni_2P single crystal atomic arrangement and surface structures. Ni_2P has the bulk structure of hexagonal Fe_2P (a = 0.59 nm, c =0.34 nm, γ=120; P -6 2 m) [18]. There are two types of phosphorus atoms occupying different positions denoted as P(1) and P(2). The P(1) atoms occupy the 1b site at (0,0,½) while the P(2) atoms occupy the 2c site at (1/3,2/3,0). There are also two kinds of nickel atoms occupying different positions, Ni(1) tetrahedrally surrounded by 4P at (0.258,0.0, 0.0) and square pyramidal Ni(2) surrounded by 5 P at (0.596 , 0.0, 0.5). There are two possible crystal truncations for the $(10\bar{1}0)$ surface. One is the $(10\bar{1}0)$ plane running between the P(1) and P(2) atoms; the other one passes between two P(2) atoms as shown in Fig.1. The former truncation plane creates two surfaces denoted as A and B. The latter gives two equivalent B planes.

Surface A is flat and contains P(1) while surface B contains P(2) and has a small periodic ripple along the $[\bar{1}2\bar{1}0]$ direction, originating from the arrangement of the Ni atoms. The amplitude of the ripple is as small as 0.075 nm. Planes A and B are stacked in a sequence of ABBABB. In both A and B surfaces the P atoms have an atomic linear configuration in the [0001] direction. The separation of P rows is 0.59 nm equal to the lattice constant $|\mathbf{a}_1|$. The P atoms are arranged exactly in the same way as the A and B surface structures. There are two types of Ni atoms (Ni(1) and Ni(2)) between the rows of P atoms.

After sputtering and annealing at 573 K, a clear LEED pattern appeared as shown in Fig.2(a). The spots corresponded well to the (1×1) surface. After annealing at 723 K, the LEED pattern changed with new spots appearing between the (1x1) spots as shown in Fig.2(b). New spots appeared on the line just half-way between the two substrate spots rows running in the $\mathbf{a}_2^*$ direction; these new spots on the row appeared at the position of 1/2 $\mathbf{a}_1$* +1/4$\mathbf{a}_2^*$ with a periodicity of $1/2|\mathbf{a}_2^*|$. The other spots appeared between the substrate spots along $\mathbf{a}_2^*$. Thus the new spots were arranged in a rhombic lattice with unit vectors $\mathbf{p}_1^*$ and $\mathbf{p}_2^*$ or in a centered rectangular lattice with vectors $\mathbf{b}_1^*$ and $\mathbf{b}_2^*$ shown in Fig.2b.

The unit vectors of the superstructure could be written as follows

$$\begin{pmatrix}\mathbf{p}_1\\ \mathbf{p}_2\end{pmatrix}=\begin{pmatrix}1 & 2\\ -1 & 2\end{pmatrix}\begin{pmatrix}\mathbf{a}_1\\ \mathbf{a}_2\end{pmatrix}$$

or

$$\begin{pmatrix}\mathbf{b}_1\\ \mathbf{b}_2\end{pmatrix}=\begin{pmatrix}2 & 0\\ 0 & 4\end{pmatrix}\begin{pmatrix}\mathbf{a}_1\\ \mathbf{a}_2\end{pmatrix}$$

We denoted the superstructure as a $c(2\times4)$ unit cell.

3.2 STM images

Fig. 3 shows the STM picture of a 50 × 50 nm^2 section of the $Ni_2P(10\bar{1}0)$ surface after annealing at 573 K. Although a (1×1) LEED pattern was observed, there were deep holes and 5-8 nm particles.

Fig. 4(a) shows the high resolution STM images obtained at a negative (-1.5 V) bias after the sample was annealed at 723 K at which conditions the $c(2\times4)$ LEED pattern was observed. There were two types of fine structured patterns. One had thin line structures running along the [0001] ($\mathbf{a}_1$) direction which were periodically separated by 0.59 nm along the $[\bar{1}2\bar{1}0]$ ($\mathbf{a}_2$) direction. The separation corresponded well to the $\mathbf{a}_2$ lattice constant. Fig. 4(b) and Fig.4(c) show the magnified image of this thin line structure and its contrast-enhanced one, respectively. Careful examination revealed that it

was composed of small dots, the separation of which corresponded to the $|\mathbf{a}_1|$ distance of 0.34 nm as shown in Fig.4(c). Thus the thin wire structure had a (1x1) structure. The position of the bright spots coincided with the locations of the P atoms on both the A and B planes of the $[10\bar{1}0]$ surface.

The upper left side of Fig. 4(a) showed the other type of structure consisting of a thick line also running parallel to the [0001] ($\mathbf{a}_1$) direction. The separation of the thick lines was twice as large as the $|\mathbf{a}_2|$ distance of 0.592 nm. It was inferred that the (1×2) structure was aligned along the [0001] direction. However, a (1×2) LEED pattern was never observed at any position of the sample. Close examination of the thick lines revealed zigzag structures as shown in Fig.4(d). The separation between the corners of the zigzag in the [0001] direction was 0.68 nm, twice as large as the $|\mathbf{a}_1|$ distance of 0.34 nm. Meanwhile, adjacent zigzag structures had an antiphase arrangement, so that the zigzag structure had a head-to-head orientation or the bright spots appeared in the same side of the thick lines. Thus the unit cell should be twice as large as the separation between the thick lines shown in Fig. 4(d), corresponding to a c (2 × 4) superstructure as was found in the LEED patterns.

What is observed in STM?

The first question that needs to be addressed is the origin of the bright spots in the STM images. Although this topic has already been discussed for the (1×1) and $\sqrt{3}\times\sqrt{3}$ surfaces of $Ni_2P(0001)$ in our previous papers,[4-6,8], it is important to consider the assignment for this work. In our previous papers the bright spots were identified to surface P atoms. The reasons were as follows,

(1) Bright spots appeared at the P atom positions expected from an ideal surface termination for a (0001) surface.
(2) DFT calculations on (0001) surface predicted that only P atoms should be visible at positive bias. [19]

Despite this evidence, the assignment of the bright spots to phosphorus atoms is not unequivocal. The STM contrast reflects not only the geometrical height but also the electronic density-of-states. Thus the position does not necessarily mean the position of atoms. In addition, atomic scale STM pictures on $Ni_2P(10\bar{1}0)$ were obtained using negative biases while the DFT calculations of the $Ni_2P(0001)$ surface predict both Ni and P atoms should be visible in the negative biases.[19]

Preliminary DFT calculations were carried out on the unreconstructed surface $(10\bar{1}0)$ for the negative bias case without considering surface relaxation. Fig. 5 shows the local electron density-of-states 0.25 nm above plane A of the $(10\bar{1}0)$ surface. We found that the P site has a higher density-of-states and the P atoms appeared brighter than the Ni atoms even at negative bias on the $Ni_2P(10\bar{1}0)$. This calculation result agrees with the assignment that the P was observed in STM measurement at negative bias.

Although more elaborate DFT calculations including surface relaxation and possible

reconstruction must be performed to interpret the STM images, the further analysis of the images presumes that P atoms were visible in the $(10\bar{1}0)$ surfaces for both the (1×1) and c (2×4) structures.

First the unreconstructed (1×1) surface is considered. On this surface the P-P distance along the [0001] direction is 0.34 nm and along the $[\bar{1}2\bar{1}0]$ is 0.59 nm to which the bright spots observed in the STM image corresponded well.

Next the model structure for the c (2×4) surface is considered. The bright zigzag structure observed in the STM image as shown in Fig. 4d was presumed to be due to P atoms. Comparing the bright spots and the Ni_2P $(10\bar{1}0)$ surface directly, the c (2×4) pattern was simply related to the structure where a P dimer was alternatively removed from the surface as shown in Fig. 6(a,b). We called the structure as the missing-dimer model (MDM). However, there are several problems with the MDM. According to this model the surface density of P atoms should be lower by a half than that of the (1×1) surface as shown in Fig.4(c). This means that the P atom separation should be larger than that in the (1×1) structure so that each P atom in the c(2 × 4) structure should be individually visible. However, single P atoms could not be observed. Instead, thick lines or large strands with zigzag patterns were present. Thus, it is concluded that the phosphorus should be more densely packed on the real-space c (2×4) surface. Another problem was the modulation of the height. The height modulation of the (1×1) domain was small (only 0.02 nm) while that on the c (2×4) was as large as 0.10 nm. In addition to that the P-dimer defect site corresponded to a bright feature according to the MDM. For these reasons the MDM was discarded.

Another possible structure that gives a c(2 x 4) structure is a missing-row model (MRM), depicted in Fig. 6(c,d). The Ni_2P $(10\bar{1}0)$ surface can be regarded as one-dimensional structure where P and two Ni rows run along the [0001] direction. In analogy to the Pt(110) surface, the removal of every other two Ni rows along the [0001] direction as shown in Fig. 6, in addition to the removal of a P dimer in the same manner as in the MDM, produces a c(2 × 4) structure and the zigzag arrangement. The removal of P atoms can be rationalized by the need to conserve a Ni to P atomic ratio of 2:1. The removal of every other two Ni rows corresponds to 1 Ni atom missing from the unit cell, while the removal of the P dimer correspond to 0.5 P atom missing from the unit cell. This MRM could explain the large vertical modulation of the c(2 × 4) surface. This MRM might be stable because it maintains the 2:1 stoichiometry. However, a problem is that the MRM cannot explain the presence of the bright strand which requires higher P atom density than that on the (1×1) surface. Another model structure must be considered.

The driving force to create the (1×2) reconstruction in Pt(110) is to realize the most stable and densely packed surface on the slope of the Pt rows. In the MRM of the $Ni_2P(10\bar{1}0)$ surface the

slope is composed of $(11\bar{2}0)$ and $(2\bar{1}\bar{1}0)$ surfaces. The $(11\bar{2}0)$ and $(2\bar{1}\bar{1}0)$ surfaces are polar surfaces where only P or Ni is exposed. If Ni and P are fully ionized, both surfaces should not be stable. However, if the covalence in Ni-P bonds is larger than the ionic character, the situation would be different. The Ni d orbitals are not fully occupied and can have unpaired dangling bonds on the surface. These dangling bonds are potentially capable of further bonding. In contrast the P atoms have an s^2p^3 configuration and undergo sp^3 hybridization. Each P atom is bound to 3 Ni atoms with 3 sp^3-hybridized orbitals which forms the highest occupied molecular orbital (HOMO) bond. Another sp^3-hybridized orbital is oriented upwards which is fully filled. Consequently no more dangling bonds are left on the P-terminated surface. This reconstruction scheme is similar to that found in the GaAs(001) surface where As with filled dangling bonds tends to cover the surface.[12,13] If this assumption is correct, A P atom row should be possible to put on the thick bright lines where the Ni atoms are exposed as shown in Fig. 7 (a) in order to terminate the surface completely with saturated P atoms as shown in Fig. 7(b). This model is called as the Ni missing-row and P added-row model (MRARM). The added P row and the original surface P atoms shown in arrows are visible and compose the opposite zigzag structure denoted as a white line as shown in Fig.7(c). This model has the following desirable features.

1. The height modulation is large.
2. All the Ni atoms are covered by P atoms. The Ni site under the missing P atoms is still bonded to the second nearest P atom with a P-Ni bond distance of 0.246 nm.
3. The surface density of P atoms becomes larger in the bright thick lines as observed in the STM image.

From this study we present a possible general principle for the surface reconstruction of Ni_2P. "*Nickel phosphide surfaces are stabilized by P-termination which eliminates the dangling bonds on the nickel atoms.*" In metal-rich TM compounds, the transition metal-main group element bond becomes more covalent as the metal content increases [20]. Thus, the bonding between the metal- and main group element is more covalent and may follow the reconstruction trends observed in compound semiconductors in which bond rearrangements occur to reduce the number of dangling bonds.

The results of this study provides some understanding for catalysis on nickel phosphide. Although Liu et al. has found that P in phorsphide plays a role to activate the catalysis through both ligand and ensemble effects,[21,22] it is expected that phosphorus termination will eliminate the coordinatively unsaturated sites on the metal atoms, which are the positions for chemical bond formation with reactants. Meanwhile, the phosphorus layer will also provide protection for the bulk material in the commonly employed procedure of passivation, where the freshly synthesized material is exposed to a dilute stream of oxygen to allow handling at ambient conditions[23]. Thus, in the

majority of studies the nickel phosphide is reduced at high temperature prior to reaction to remove the passivation layer, and this probably also removes some of the surface phosphorus to expose metallic sites and render the catalyst active. This surface science work has provided the new insight into the activation process of the phosphide catalyst.

4. Acknowledgment

The work was financially supported by Grand-in-Aids for scientific Research Category S from JSPS(No. 16106010) and the US Department of Energy, Office of Basic Energy Sciences, through Grant DE-FG02-963414669. One of the authors (D.-H.Guo) was supported by a GCOE program "Catalysis as the Basis for Innovation in Materials Science" of MEXT.

5. References

[1] S.T. Oyama, J.Catal. 216 (2003) 343.

[2] S.T. Oyama, T. Gott, H. Zhao, Y.-K. Lee, Catal. Today, 143 (2009) 94.

[3] D. Kanama, S.T. Oyama, S. Otani, D.F. Cox, Surf.Sci. 552 (2004) 8.

[4] M.G. Moula, S. Suzuki, W.J. Chun, S. Otani, S.T. Oyama, K. Asakura, Chem.Lett 35 (2006) 90.

[5] M.G. Moula, S. Suzuki, W.J. Chun, S.T. Oyama, K. Asakura, S. Otani, Surface and Interface Analysis 38 (2006) 1611.

[6] K. Kinoshita, G.H. Simon, T. Konig, M. Heyde, H.J. Freund, Y. Nakagawa, S. Suzuki, W.-J. Chun, , S.T. Oyama, S. Otani, K. Asakura, Jpn.J.Appl.Phys. 47 (2008) 6088.

[7] K. Edamoto, Y. Nakadai, H. Inomata, K. Ozawsa, S. Otani, Solid State Commun. 148 (2008) 135.

[8] S. Suzuki, G.M. Moula, T. Miyamoto, Y. Nakagawa, K. Kinosthita, K. Asakura, S.T. Oyama, S. Otani, J. Nanosci. and Nanotech. 9 (2009) 195.

[9] K. Edamoto, H. Inomata, T. Shimada, K.-i. Ozawa, S. Otani, e-J. Surf. Sci. and Nanotech. 7 (2009) 1.

[10] V. Fiorentini, M. Methfessel, M. Scheffler, Phys Rev Lett 71 (1993) 1051.

[11] C. Noguera, J.Phys.Cond.Matter 12 (2000) R367.

[12] C.B. Duke, Chem. Rev. 96 (1996) 1237.

[13] A. Ohtake, Surf. Sci. Rep. 63 (2008) 295.

[14] M.D. Pashley, Phys. Rev. B 40 (1989) 10481.

[15] J. Tersoff, D.R. Hamann, Phys. Rev. B 31 (1985) 805.

[16] P. Blaha, K. Schwarz, G. K. H. Madsen, D. Kvasnicka, and J.Luitz, WIEN2k, An Augmented Plane Wave Plus Local Orbitals Program for Calculating Crystal Properties (Vienna University of Technology, Austria, 2001).

[17] G. K. H. Madsen, P. Blaha, K. Schwarz, E. Sjöstedt, and L. Nordström, Phys. Rev. B 64 (2001) 195134.

[18] S. Rundqvist, Acta Chem. Scand. 16(1962) 992.

[19] Q. Li, X. Hu, Phys. Rev. B 74 (2006) 035414.

[20] P.E.R. Blanchard, A.P. Grosvenor, R.G. Cavell, A. Mar, Chem. Mater. 20 (2009) 7081.

[21] P. Liu, J.A. Rodriguez, T. Asakura, J. Gomes, K. Nakamura, J. Phys. Chem. B 109 (2005) 4575.

[22] P. Liu, J.A. Rodriguez, J. Am. Chem. Soc. 127 (2009) 14871.

[23] X. Wang, Y. Lee, S.T. Oyama, K. Bando, F.G. Requejo, J. Catal. 210 (2002) 207.

Figure Captions:

Fig. 1 Crystal structure, directions and planes. (a) Hexagonal crystal structure of Ni_2P;(b) Layers normal to the $(10\bar{1}0)$ surface along the [0001] direction(Plane A terminated);(c) top view of "A plane" of the $(10\bar{1}0)$ surface and (d) that of "B plane ".

Fig. 2 LEED pattern from the Ni_2P $(10\bar{1}0)$ surface. Electron energy is 70 eV. (a) primitive (1 x 1) structure. (b) c(2x4) structure. $\mathbf{a_1}^*$ and $\mathbf{a_2}^*$ are reciprocal unit vectors for primitive (1×1) cell while $\mathbf{p_1}^*$ and $\mathbf{p_2}^*$ are those for reconstructed surface. $\mathbf{b_1}^*$ and $\mathbf{b_2}^*$ are the unit vectors for rectangular unit cell of $c(2\times4)$.

Fig. 3 STM image of the Ni_2P $(10\bar{1}0)$ surface after annealing at 573 K. (Vs=2.5 V, It=100 pA, size 50 × 50 nm^2)

Fig. 4 High resolution STM images of the Ni_2P $(10\bar{1}0)$ surface after annealing at 723 K. Vs = - 1.5 V, It = 130 pA. (a) 20 × 20 nm^2; (b) magnified image of the lower right domain of (a); (c) contrast-enhanced image of (b) ; (d) magnified image of upper left domain of (a). Rectangular in the (b), (c), and (d) is a unit cell. The white circle and the zigzag lines in (d) are eye-guides to indicate the $c(2\times4)$ structure and a head-on-head arrangement more clearly.

Fig. 5 Electron density 0.25 nm away from the surface.

Fig. 6 Model structure of the Ni_2P $(10\bar{1}0)$ surface c(2 × 4) reconstruction. (a,b) Missing dimer model (MDM); (c, d) missing row model (MRM).

Fig. 7 Model structure of the Ni_2P $(10\bar{1}0)$ c(2 × 4) surface (Missing nickel row added phosphorus row model-MRARM). (a) MRM with the arrow indicating the empty Ni sites ;(b) P atoms added on top of the empty Ni sites; (c) The top and side views of MRARM. Arrows show the visible phosphorus atoms.

Figure 1

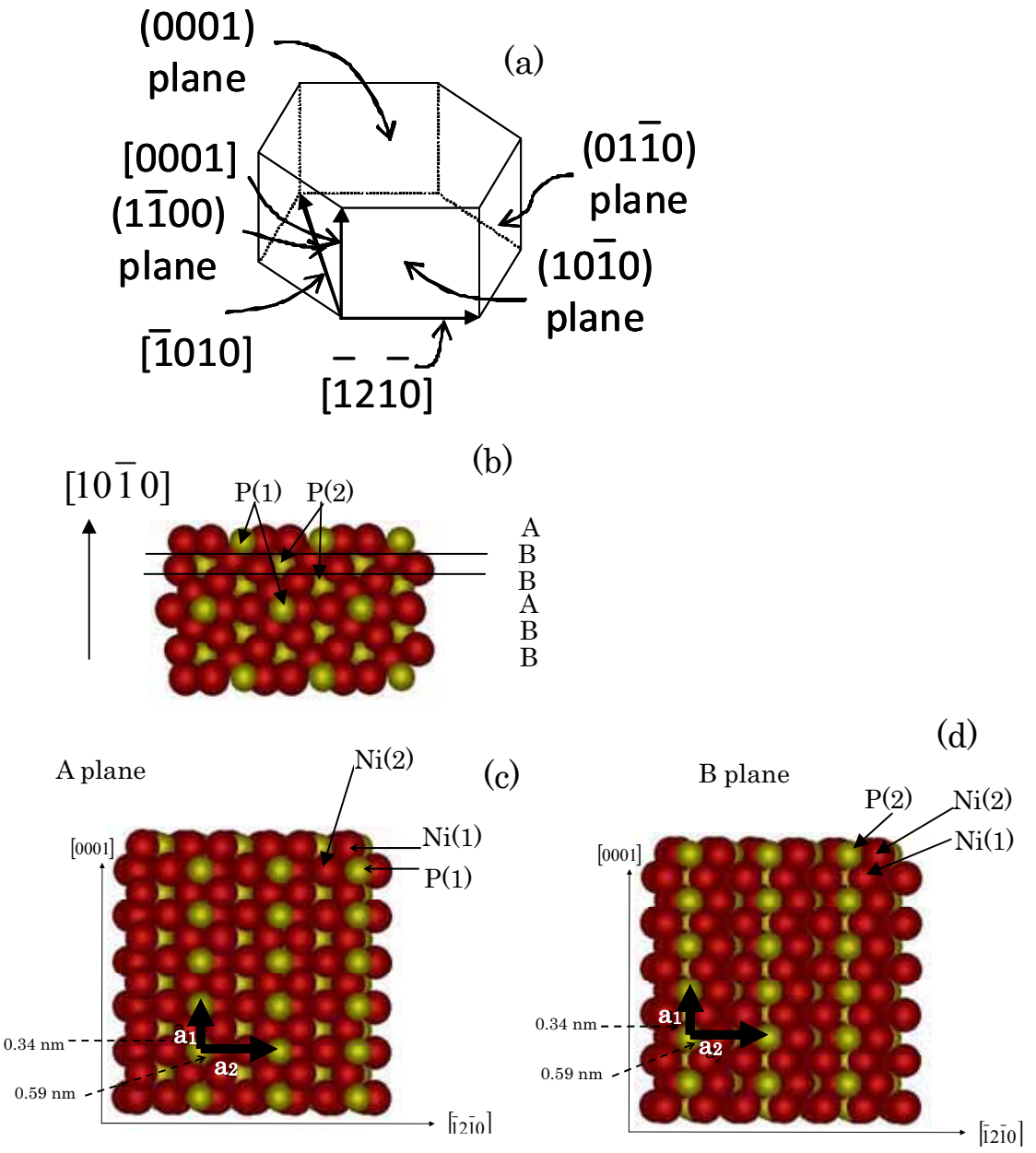

Fig.1 GUO *et al.*

Fig2

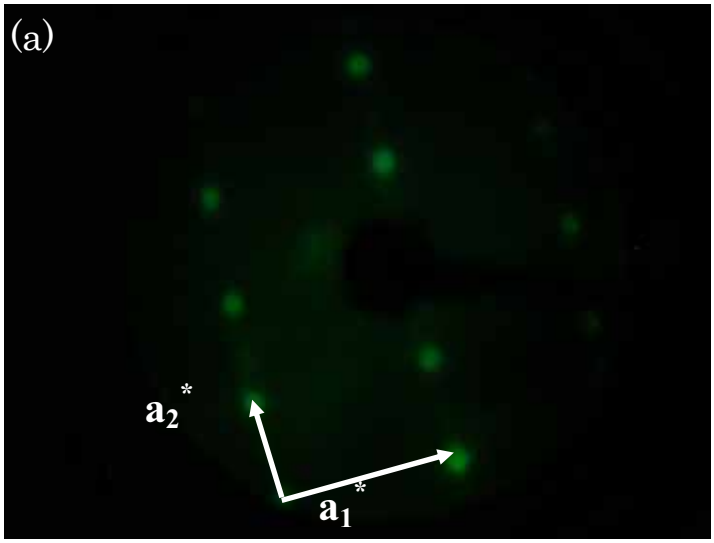

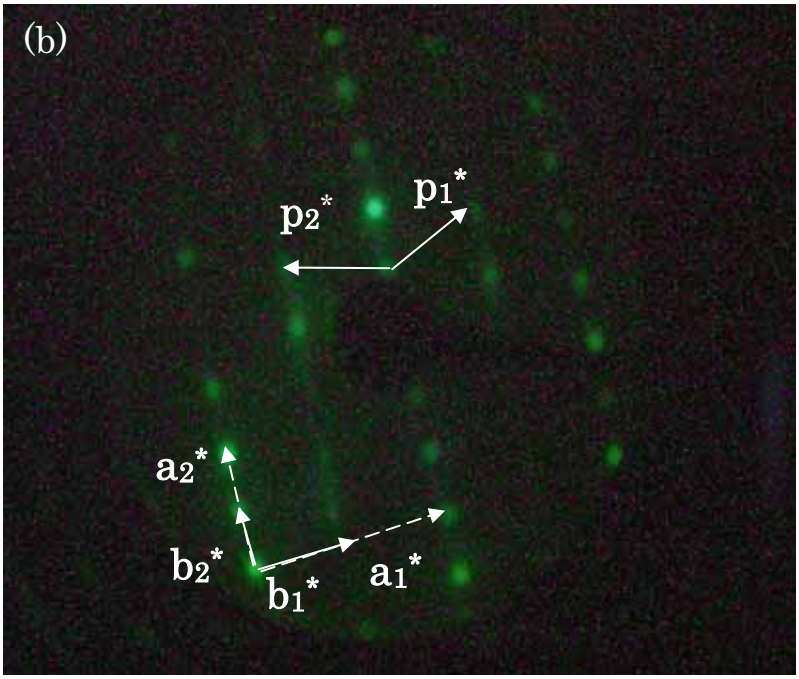

Fig.2

Fig3

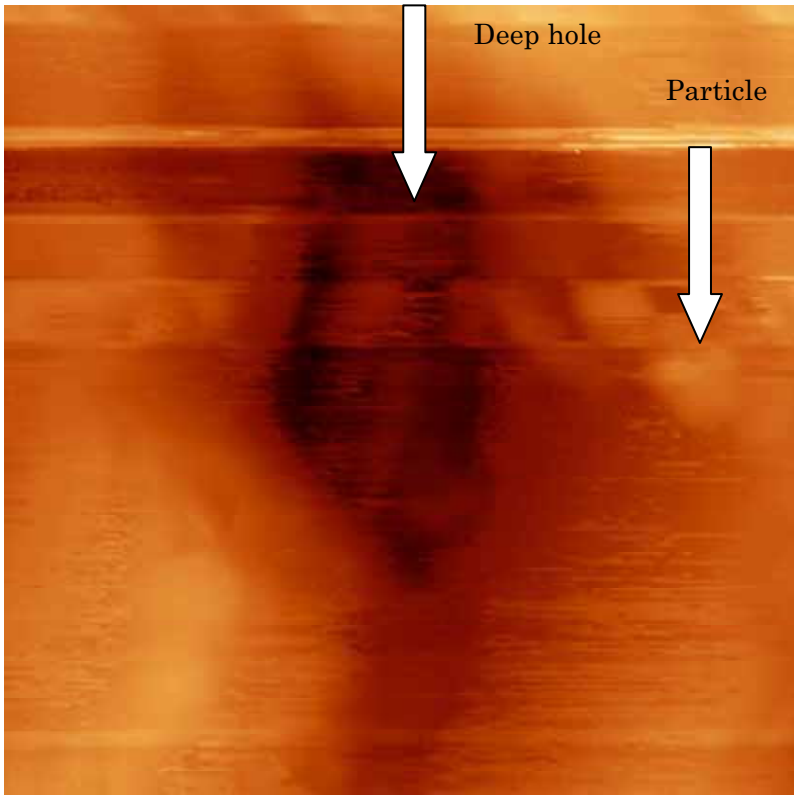

Fig.3

Figure 4

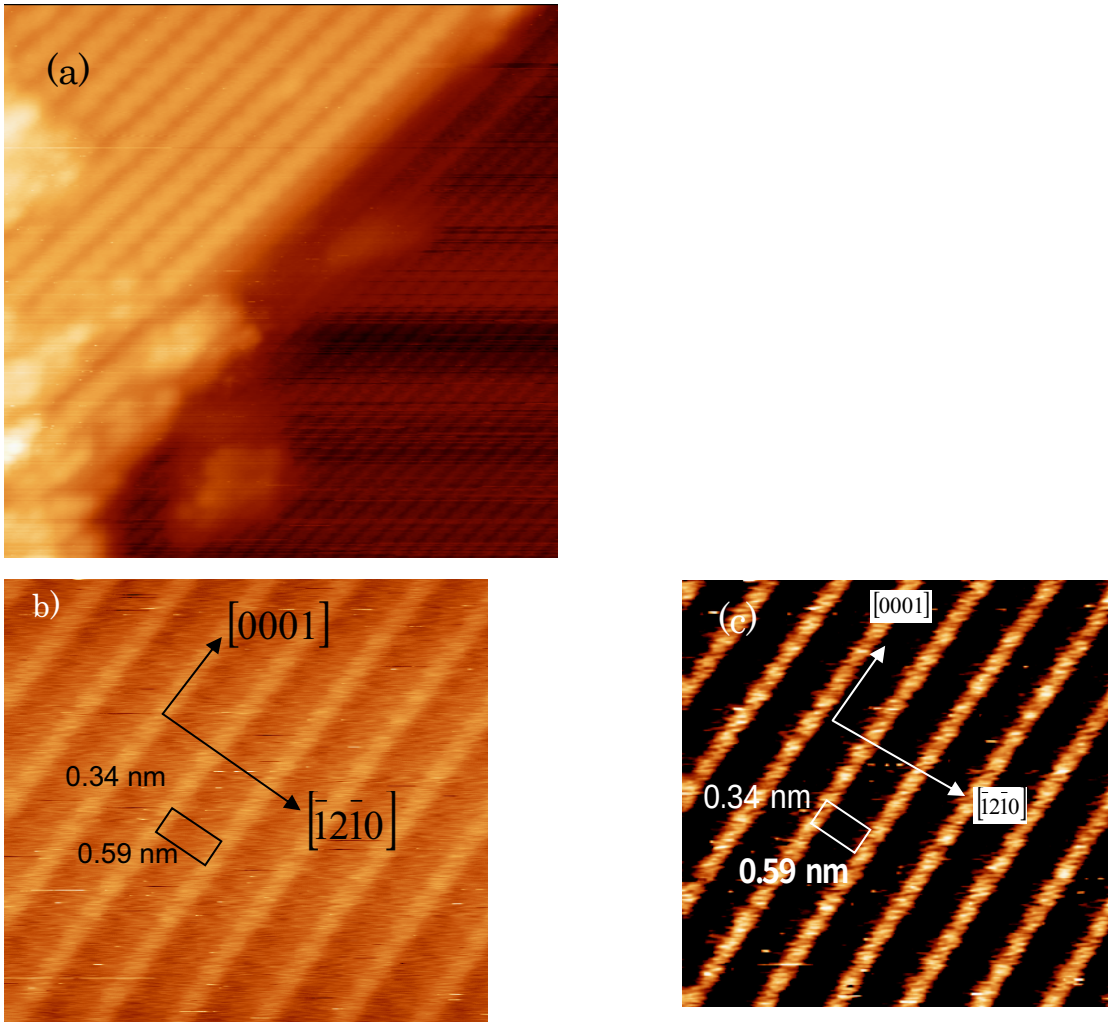

Fig. 4

Figure 5

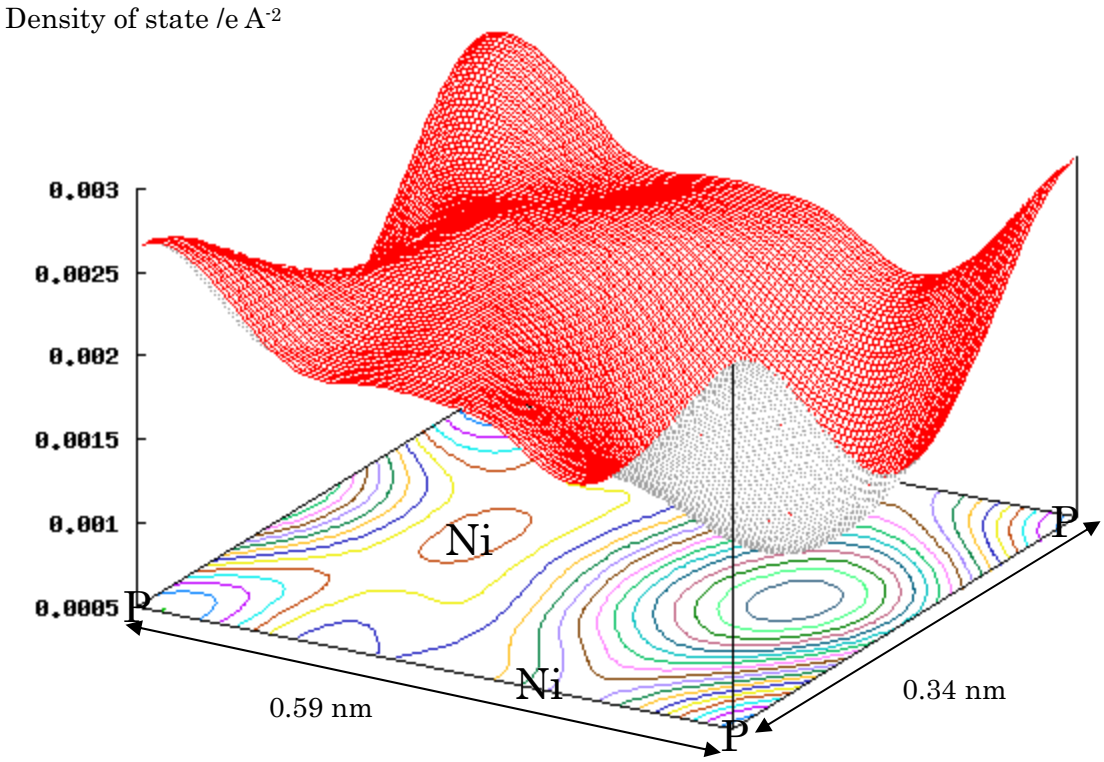

Fig.5

Figure 6

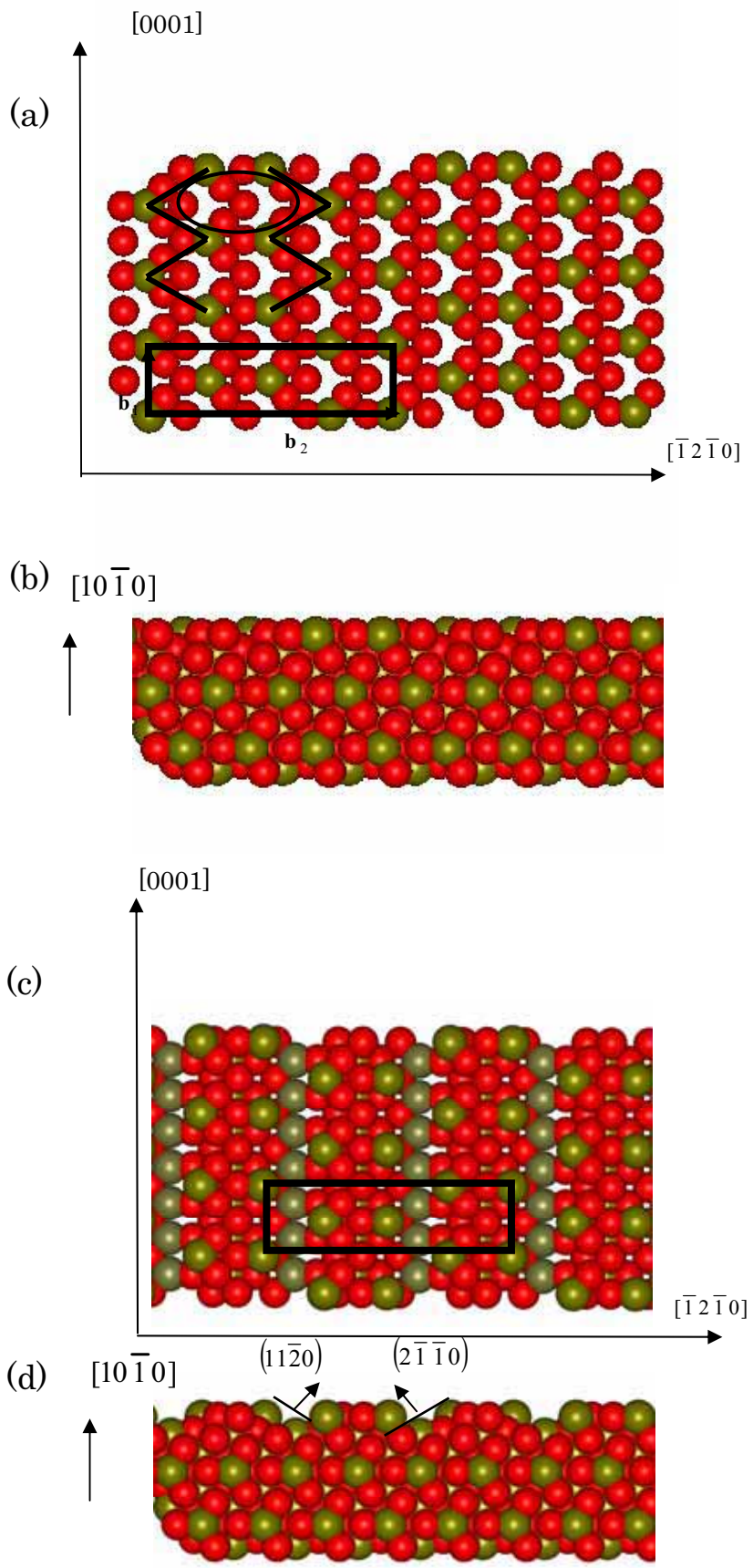

Fig.6

Figure(s)

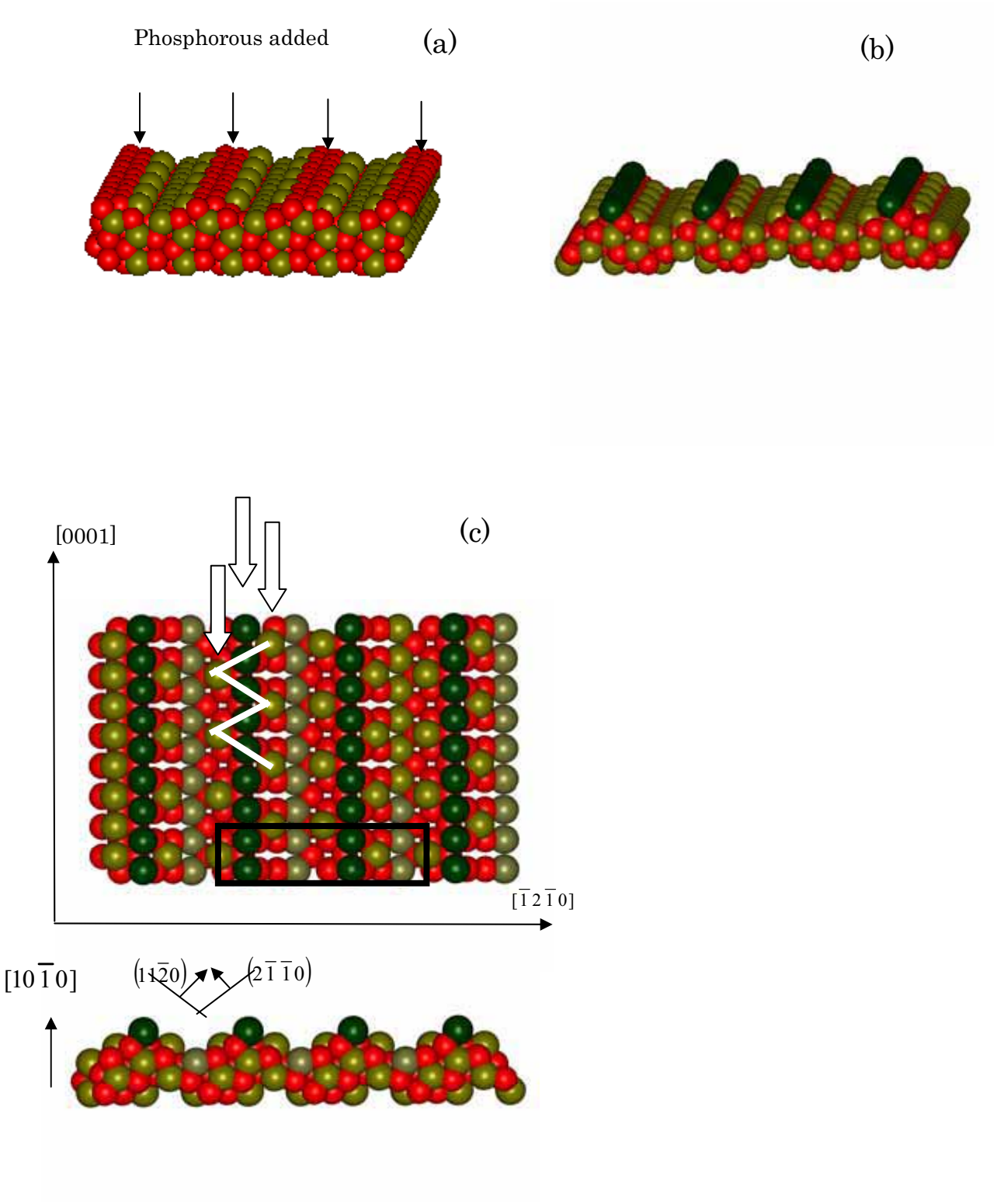

Fig.7